Comparison of the Experimental and Theoretical Structure Factors of Temperature Sensitive Polymer Gels

Mitsuhiro Shibayama,* Kazuki Kawakubo, and Tomohisa Norisuye

Department of Polymer Science and Engineering, Kyoto Institute of Technology Matsugasaki, Sakyo-ku, Kyoto 606, Japan

Received November 6, 1997; Revised Manuscript Received January 2, 1998

ABSTRACT: The comparison of the experimental and theoretical structure factors, $S(q)$, of weakly charged polymer gels has been carried out as a function of the gel parameters, i.e., temperatures at preparation and at observation, polymer concentration, and degrees of cross-linking and of polymerization, where q is the scattering vector. Experimental structure factors at two different q regimes, i.e., small-angle neutron scattering (SANS, $0.005 \leq q \leq 0.1$ Å^{-1}) and light scattering (LS, $q \approx 0.001$ Å^{-1}) regimes, were employed for the comparison with the Rabin−Panyukov (RP) theory for weakly charged gels. In the case of SANS, a quantitative agreement was obtained for $S(q)$ in the poor solvent regime. For LS, $S(q)$ was decomposed to two contributions from dynamic thermal fluctuations and static frozen inhomogeneities. The experimental results on their parameter dependence of $S(q)$ were successfully reproduced by the RP theory.

Introduction

It has been reported that the structure factor $S(q)$ of weakly charged polymer gels has a maximum at a finite q if the solvent is a poor solvent to the main constituent of the gel, where q is the magnitude of the scattering vector.[1−3] Concentration fluctuations which lead to the scattering maximum are ascribed to a balance of antagonistic interactions, i.e., the electrostatic repulsion of the charged groups and hydrophobic bonding of the main chains. The appearance of the scattering maximum was first predicted theoretically by Borue and Erukhimovich (BE) for weakly charged polyelectrolytes in a poor solvent.[4] The BE theory was successfully employed to explain the structure factor of polyelectrolyte solutions.[5] It was demonstrated that the BE theory is also applicable to weakly charged polymer gels.[3] However, the effect of cross-linking on $S(q)$ has not been fully elucidated. Recently, Panyukov and Rabin developed a comprehensive theory of polymer gels.[6,7] The characteristic feature of the Panyukov−Rabin theory is that the structure factor of polymer gels is described by two sets of parameters, i.e., those at preparation and at observation. This type of theoretical treatment allows one to predict changes in $S(q)$ for a gel subjected to various types of treatment after its preparation. Rabin and Panyukov then extended their theory for neutral gels to one for weakly charged gels by taking account of the q dependence of the electrostatic interaction, which we call hereafter the Rabin−Panyukov (RP) theory.[8]

Polymer gels have two types of concentration fluctuations.[9−12] One is liquidlike thermal fluctuations which reflect the liquidlike nature of polymer gels and are time dependent. The other is spatial frozen fluctuations introduced by cross-linking. This spatial fluctuations are time-independent but position-dependent fluctuations. Therefore, we call the latter the spatial inhomogeneities. A pioneering work on a decomposition of the two contributions by dynamic light scattering (DLS) was carried out by Candau et al. in the late 1970s,[9] where they pointed out the importance of the static inhomogeneities acting as a local oscillator in the light scattering. Joosten et al. demonstrated an elaborate method to decompose these contributions, which involves DLS measurements at a large number of positions in a sample.[13] The same method was employed by others in order to study the spatial inhomogeneities in gels.[14−17] In the previous papers,[18,19] we also demonstrated that DLS is a relevant method to decompose the static inhomogeneities from the thermal fluctuations if DLS is coupled with ensemble averaging. Then, each contribution to the scattered intensity $I(q)$, proportional to $S(q)$, has been discussed as a function of the gel parameter, such as cross-link density, temperatures at preparation and observation, and the degree of ionization.[20]

Since $S(q)$ of the RP theory consists of two correlators, i.e., the correlator of the thermal fluctuations, $G(q)$, and that of the static inhomogeneities, $C(q)$, it is of particular interest to examine the RP theory with the corresponding intensity functions obtained experimentally. By comparing the experimental results and theoretical prediction, we examine the validity of the theory in various aspects, clarify the limit of the theoretical prediction, and discuss the structure and dynamic properties of polymer gels.

Theoretical Background

1. Static Structure Factor of Weakly Charged Gels. Rabin and Panyukov (RP) developed a theory to predict the structure factor, $S(q)$, of weakly charged polymer gels.[8] This is based on the theory by Panyukov and Rabin for instantaneously cross-linked Gaussian chains with excluded volume.[6,7] The structure factor consists of two contributions, one from thermal fluctuations, $G(q)$ (the dynamic correlator), and the other from

* To whom correspondence should be addressed.

S0024-9297(97)01641-0 CCC: $15.00
Published on Web 02/13/1998

static density inhomogeneities, $C(q)$ (the static correlator)

$$S(q) \equiv \overline{\langle \rho(q)\rho(-q)\rangle} = G(q) + C(q) \quad (1)$$

$$G(q) \equiv \langle \rho(q)\rho(-q)\rangle = \langle \rho^{th}(q)\rho^{th}(-q)\rangle \quad (2)$$

$$C(q) \equiv \overline{\rho^{eq}(q)\rho^{eq}(-q)} \quad (3)$$

where $\rho^{eq}(q)$, $\rho^{th}(q)$, and $\rho(q)$ are the Fourier components of the equilibrium density variations, of the thermal density fluctuations, and of the total density variations, respectively. Thus,

$$\rho(q) \equiv \rho^{eq}(q) + \rho^{th}(q) \quad (4)$$

There are two types of averages here: the structure (ensemble) average denoted by a bar over the variable and the thermal average given by $\langle\ \rangle$, where $\rho(q)$ is the Fourier component of the density variation. Note that $\rho^{eq}(q)$ minimizes the free energy of the gel and has the following properties; $\langle \rho^{eq}(q)\rangle \neq 0$ and $\overline{\rho^{eq}(q)} = 0$. For weakly charged gels in the absence of salt ions, $G(q)$ and $C(q)$ are given by

$$G(q) = \frac{\phi N g(q)}{1 + w(q)g(q)} \quad (5)$$

$$C(q) = \frac{\phi \mathrm{N}}{[1 + w(q)g(q)]^2(1 + Q^2)^2} \times \left[6 + \frac{9}{w_0(q) - 1 + (1/2)Q^2(\phi_0/\phi)^{2/3}\phi_0^{-1/4}}\right] \quad (6)$$

where N, ϕ, and ϕ_0 denote the average degree of polymerization between cross-linking points and the polymer volume fractions at observation and at preparation, respectively. Note that the $G(q)$ and $C(q)$ in eqs 5 and 6 are dimensionless while those in the original theory have the unit of inverse of the segment volume, i.e., a^{-3} with a being the segment length. Q is defined as the dimensionless wave vector by

$$Q = aN^{1/2}q \quad (7)$$

It should be noted here that the $G(q)$ and $C(q)$ are coupled with the function $g(q)$, which is given by

$$g(q) = \frac{1}{Q^2/2 + (4Q^2)^{-1} + 1} + \frac{2(\phi/\phi_0)^{2/3}\phi_0^{1/4}}{(1 + Q^2)^2} \quad (8)$$

The effect of charges appears in the dimensionless net-excluded volume parameter, which becomes q-dependent

$$w(q) = (1 - 2\chi + \phi)\phi N + \frac{\hat{l}_B f^2 \phi N^2}{Q^2 + \hat{l}_B f \phi N} \quad (9)$$

$$w_0(q) = \phi_0^{5/4}N + \frac{\hat{l}_B f_0^{\,2}\phi_0^{5/4}N^2}{Q^2(\phi_0/\phi)^{2/3} + \hat{l}_B f_0 \phi_0^{5/4}N} \quad (10)$$

where $\hat{l}_B$ is the dimensionless Bjerrum length defined by

$$\hat{l}_B = 4\pi l_B/a \quad (11)$$

and χ is the Flory−Huggins interaction parameter. l_B is the Bjerrum length (≈7 Å for aqueous solutions at 25 °C). f and f_0 are the degrees of ionization at observation and at preparation, respectively. In this study, we do not consider the effect of salt ions although the original theory takes into account of this contribution.[8] This is due to the fact that the effect of salt ions appears both in $w(q)$ and $w_0(q)$ with the same magnitude for reactor-batch gels. As a result, the net effect in the correlator becomes insignificant. Even ignoring the salt ion concentration, the RP theory has many parameters. However, most of them can be fixed by the experimental conditions, particularly for the parameters at preparation, e.g., ϕ_0, f_0, and N, and some at observation, e.g., ϕ and f. Therefore, the curve fitting of an observed intensity function $I(q)$ with the theoretical structure factor $S(q)$ can be carried out with a few floating parameters, e.g, χ and the intensity scale factor, K, where

$$I(q) = KS(q) \quad (12)$$

Theoretically, the intensity scale factor can be calculated if $I(q)$ is obtained in the absolute intensity scale. In this case, K is given by[21]

$$K = \frac{N_A}{v_B}\left[b_A\left(\frac{v_B}{v_A}\right) - b_B\right]^2 \quad (13)$$

where N_A is the Avogadro's number, and v_i and b_i are the molar segment volume and the scattering length of the component i, respectively.

2. Decomposition of $S(q)$ to Two Contributions from Dynamic Fluctuations and Static Inhomogeneities. In the case of polymer gels, the intensity−intensity time correlation function, $g^{(2)}(\tau)$ is obtained by DLS measurements and, in many cases, $g^{(2)}(\tau)$ can be fitted with a single-exponential function with an apparent cooperative diffusion coefficient, D_A.[22] However, the scattered intensity depends strongly on the sample position due to the nonergodicity of gels.[12,13] According to Joosten et al.,[13] the following relation holds for polymer gels

$$D_A = \frac{D}{2 - \langle I_F(q)\rangle_T/\langle I(q)\rangle_T} \quad (14)$$

where D is the cooperative diffusion coefficient of the gel, $\langle I(q)\rangle_T$ is the time-average scattered intensity, and $\langle I_F(q)\rangle_T$ is the dynamic component of $\langle I(q)\rangle_T$. By rearranging eq 14, one obtains

$$\frac{\langle I(q)\rangle_T}{D_A} = \frac{2}{D}\langle I(q)\rangle_T - \frac{\langle I_F(q)\rangle_T}{D} \quad (15)$$

Therefore, by plotting $\langle I(q)\rangle_T/D_A$ as a function of $\langle I(q)\rangle_T$, both $\langle I_F(q)\rangle_T$ and D can be evaluated from the intercept and the slope, respectively. Hence the ensemble-average intensity component due to the static inhomogeneities, $\langle I_C(q)\rangle_E$, is given by

$$\langle I_C(q)\rangle_E \equiv \langle I(q) - \langle I_F(q)\rangle_T\rangle_E = \langle I(q)\rangle_E - \langle I_F(q)\rangle_T \quad (16)$$

where $\langle I\rangle_E$ is the ensemble average of the scattered intensity.

Experimental Section

Samples. Poly(*N*-isopropylacrylamide) (NIPA) homopolymer gels and poly(*N*-isopropylacrylamide-*co*-acrylic acid) (NIPA/

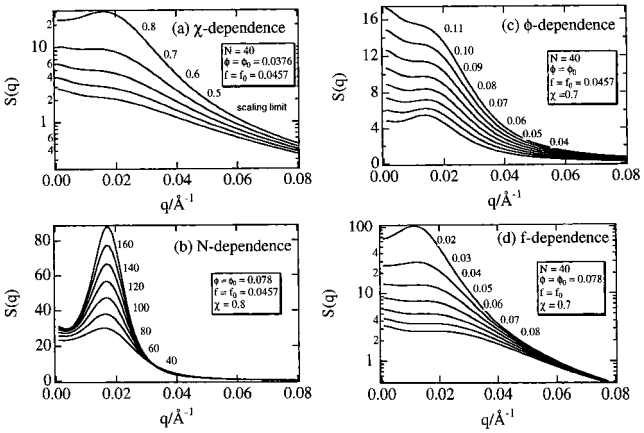

Figure 1. Parameter dependence of the theoretical structure factor, $S(q)$: (a) χ (Flory−Huggins interaction parameter), (b) N (average degree of polymerization between cross-links), (c) ϕ (volume fraction of the network), and (d) f (degree of ionization) dependence. Numbers next to curves indicated the values of the parameter. Fixed parameters are shown in the inset.

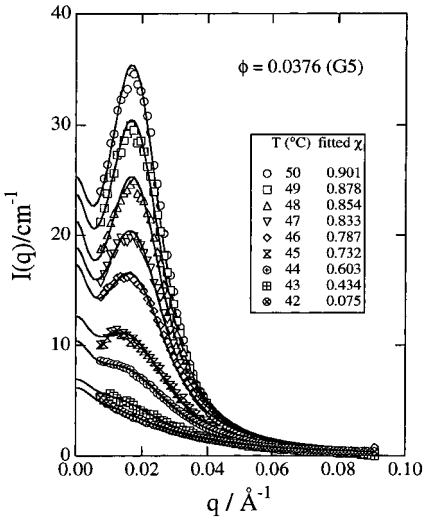

Figure 2. Observed SANS scattered intensity functions, $I(q)$, for NIPA/AAc gels (G5; $\phi = 0.0376$) at temperatures from 42 to 50 °C (symbols) and fitted structure factors (solid lines). The fitted values of χ are tabulated in the inset.

AAc) copolymer gels were prepared by redox polymerization. NIPA and NIPA/AAc gels were synthesized at 20 °C from NIPA monomer solutions and monomer mixture solutions of NIPA and AAc, respectively, in the presence of *N*,*N*,*N*′,*N*′-tetramethylethylenediamine (TEMED; accelerator), *N*,*N*′-methylenebis(acrylamide) (BIS; cross-linker), and ammonium persulfate (initiator). The details of sample preparation are described elsewhere.[3,18] The standard recipe was 668 mM of NIPA, 32 mM of AAc, and 8.62 mM of BIS. Samples for the SANS experiment were prepared in deuterated water. The gel was smashed with a sieve, followed by drying. Then a given amount of deuterated water was added to the dried gel. On the other hand, for DLS measurements, reactor-batch gels prepared in a 10 mm-diameter test tube were used without further treatment. For the parameter dependence experiments for the DLS measurement, one of the parameters was changed by keeping the others unchanged.[19]

SANS. Small-angle neutron scattering (SANS) experiments were conducted at the Research Reactor at the National Institute of Standard and Technology, Maryland. Gel samples immersed in deuterated water were sealed in a quartz cell having quartz windows and were mounted in a thermostated chamber. The samples were irradiated by a 9 Å neutron beam, and the scattered intensity was corrected for air scattering, incoherent scattering, and fast neutrons and then re-scaled to the absolute intensity. Typical exposure time was 30 min. The details of the experiment are described elsewhere.[3]

Dynamic Light Scattering. Dynamic light scattering (DLS) studies were carried out with a laboratory made optics with a photon correlator, DLS-7000, Otsuka Electric Co. The wavelength of the laser beam was 6328 Å and the scattering angle was 60°. The q value is estimated to be 0.00131 Å^{-1} according to $q = 4n\pi \sin(\theta/2)/\lambda$, where n, θ, and λ are the refractive index of the solvent ($n = 1.332$ for water at 20 °C), the scattering angle, and the wavelength of the laser in a vacuum. To simplify the problem, we use the value of $S(q)$ at $q = 0.001$ Å^{-1} for the comparison with the scattered intensity $I(q)$ obtained by LS. It should also be noted that, in addition to the conventional time correlation measurements, the ensemble average of the scattered intensity was taken in order to decompose the contribution of the static inhomogeneities.[18,23]

Results and Discussion

Parameter Dependence of the Theoretical Structure Factor. Figure 1 shows the (a) χ (Flory−Huggins interaction parameter), (b) N (average degree of polymerization between cross-links), (c) ϕ (volume fraction of the network), and (d) f (degree of ionization) dependence of the theoretical structure factor, $S(q)$, for the typical q regime of SANS, i.e., $q \leq 0.08$ Å^{-1}. The segment length was set to be $a = 8.12$ Å, which is for NIPA polymer chains.[3,24] The default values of the parameters are fixed to be $N = 40$, $\phi = \phi_0 = 0.078$, $f = f_0 = 0.0457$, and $\chi = 0.7$ (except for part b), which were chosen to match the experimental conditions. For example, N was estimated to be the ratio of the monomer concentrations of NIPA and BIS by taking account of the tetrafunctionality of BIS, i.e., $N = 700/(8.62 \times 2) \approx 40$. It is clear from these figures that most of $S(q)$'s have a single peak around $q = 0.02$ Å^{-1} for $f = f_0 = 0.0457$. The peak intensity increases with increasing, χ, N, and ϕ. The behavior shown in parts a−c of Figure 1 seems to be general. Regarding the χ dependence, it should be noted here that in the case of a good solvent regime, i.e., $\chi \ll 0.5$, $S(q)$ has to be calculated with the equation

$$w(q) = \phi^{5/4}N + \frac{l_B f^2 \phi^{5/4} N^2}{Q^2 + l_B f \phi^{5/4} N} \quad \text{(scaling limit)} \qquad (17)$$

instead of eq 9, which is given by assuming the scaling limit. Surprisingly, $S(q)$ has a scattering maximum even in the good solvent regime (i.e., the scaling regime) as shown in Figure 1a. This is one of the unique features of the RP theory. Another interesting aspect has been found in the N dependence of $S(q)$ by numerical evaluation of the RP theory. We have recently found the opposite tendency in $S(q)$ with respect to N.[25−27] Across a critical value of χ, the N dependence of $S(q)$ changes. Since the critical value lies near $\chi = 0.7$, we employed $\chi = 0.8$ in order to avoid such complexity in Figure 1b. Figure 1d indicates that the peak shifts toward a higher q region by increasing f and the peak intensity is strongly suppressed. Note that $S(q)$ is plotted by semilogarithmic scale. Since the value of f can be estimated by the preparation condition, it can be deduced that the peak position is determined mainly by the value of f and the shape of $S(q)$ can be manipulated by χ.

SANS Profiles. Figure 2 shows the observed scattered intensity functions, $I(q)$, for NIPA/AAc gels (G5; $\phi = 0.0376$) at temperatures from 42 to 50 °C (symbols).

$I(q)$ is a monotonically decreasing function with q at low temperatures (in this case for $T \leq 42$ °C) as already reported elsewhere.[3] However, as shown in this figure, $I(q)$ starts to have a peak around $q = 0.02$ Å^{-1} at $T \geq 44$ °C and $I(q)$ increases with increasing temperature. The solid curves are the calculated structure factors, $S(q)$, by using the RP theory with two fitting parameters, i.e., the intensity scale factor K and the interaction parameter χ (with eq 9), while N was fixed to be 40. The fitting seems to be satisfactory at all temperatures. This result should be compared with the work done before, i.e., Figure 11 in the previous work,[3] where the curve fitting was conducted with the Borue−Erukhimovich (BE) theory[4] for weakly charged polyelectrolytes. In the analysis with the BE theory, the following equation was employed:

$$S(x) = \frac{x^2 + s}{(x^2 + t)(x^2 + s) + 1} \tag{18}$$

x, t, and s are the reduced q vector, the reduced temperature, and the reduced charge concentration, respectively. Three parameters, i.e., K, t, and s, had to be floated in the analysis, although t and s could be estimated from the conditions of the sample preparation. There appeared a significant deviation of the fitted values from the calculated values as extensively discussed elsewhere.[28] Therefore, it is clear that the quality of curve fitting with the RP theory is much better than that with the BE theory. One of the reasons is the employment of the BE theory to the case of polymer gels, though the BE theory was developed not for polymer gels but for weakly charged polymer solutions.

The fitted values of χ are also tabulated in Figure 2. It should be noted here that the evaluated value of χ for $T = 42$ °C is much smaller than it should be. On the other hand, the evaluated values of χ seem to be satisfactory at $T \geq 44$ °C. A similar result was obtained for a gel with ϕ (=0.0127). It is shown in Figure 1a that the theoretical structure factor predicts a presence of a shoulder even for $\chi < 0.5$, i.e., even in the good solvent regime (i.e., the scaling limit regime that was characterized by eq 17). This means that the concentration profile of the polymer−solvent system is perturbed simply by introducing cross-links. The theoretical reason for the shoulder is that in a good solvent $C(q)$ decays faster with q than $G(q)$ (the characteristic length scale for decay is the inverse mesh size in the former case and the inverse thermal correlation length in the latter case). The combination of the two should have a shoulder between these two characteristic wavevectors. Such a shoulder was not observed experimentally for weakly charged gels at low temperatures (in this particular case, $T \leq 42$ °C).[3] This contradiction may be the reason why the fitting procedure produces an extraordinarily small value of χ for $I(q)$ at $T \leq 42$ °C. By comparison of these structure factors with Figure 2, it is clear why the fitting is not successful for low χ's ($\leq$0.5).

Here, we discuss the value of the parameter K for NIPA/AAc in deuterated water (water-d). Since the content of AAc is rather small, we assume a two component system with NIPA and water-d and employ eq 13. By substituting $v_A = v_{\text{water-}d} = 18.2$ cm^3, $v_B = v_{\text{NIPA}} = 102.87$ cm^3, $b_A = b_{\text{water-}d} = 19.18 \times 10^{-13}$ cm, and $b_B = b_{\text{NIPA}} = 14.03 \times 10^{-13}$ cm, K is obtained to be 0.521 cm^{-1}. The fitted values of K, however, were in the range 2.05−3.25 cm^{-1}, depending on the temperature and the polymer concentration. Therefore the difference of the factors is about four to six times. This discrepancy may be explained with a reevaluation of the value of N since N is proportional to $S(q)$. Another reason may be the effect of salt ions present in the system, which also strongly affects the scattered intensity.[29] However, a plausible reason for this discrepancy has not been obtained yet.

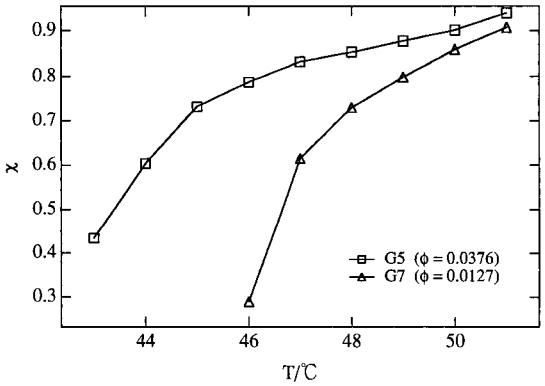

Figure 3. Temperature dependence of χ for NIPA/AAc gels having different polymer concentrations, i.e., G5 ($\phi = 0.0376$) and G7 ($\phi = 0.0127$). Lines are drawn for the eye.

Figure 3 shows the temperature dependence of χ for NIPA/AAc gels having different polymer concentrations, i.e., G5 ($\phi = 0.0376$) and G7 ($\phi = 0.0127$). The temperature and polymer concentration dependence of χ seems to be reasonable, i.e., χ is an increasing function of T and ϕ. However, the curve fitting with the RP theory was found to be unsuccessful for gels with larger values of ϕ (=0.196 and 0.107). In these cases, even the maximum q position (q_m) could not be fitted. The predicted q_m position lies much larger than the observed one. The reason for this disagreement is not clear at this stage.

Light Scattering. Figure 4a shows the variation of $I(q)$ for a set of NIPA neutral gels having different cross-link densities.[18] These gels were prepared at 20 °C. The variable r is defined as the molar ratio of the cross-linkers (BIS) to the constituent monomers (NIPA), i.e., $r \equiv C_{\text{BIS}}/C_{\text{NIPA}}$, where C_{NIPA} was fixed to be 690 mM. As shown in the figure, both $\langle I \rangle_E$ and $\langle I_C \rangle_E$ increase with r, while $\langle I_F \rangle_T$ remains rather constant with respect to r. This means that the static inhomogeneities increase with increasing cross-link density. The invariance of $\langle I_F \rangle_T$ suggests that the dynamic fluctuations, i.e., the thermal concentration fluctuations, are not affected by introducing cross-links in this cross-link density region. However, it is expected that $\langle I_F \rangle_T$ may decrease by further increasing r. Experiments along this line could not be conducted because those gels became opaque due to cross-linking-induced phase separation. Figure 4b shows the result of the theoretical prediction by the RP theory, where the following parameters were used: $f = f_0 = 0$, $\phi = \phi_0 = 0.078$, and $N = 1/r$. Note that no adjustable parameter was used and the values of N and ϕ_0 are simply calculated by stoichiometry. It is noteworthy to point out that $G(q)$ is a decreasing function of r, which indicates the dynamic fluctuations are suppressed by increasing cross-link density. By comparing parts a and b of Figure 4, it is clear that the r dependence of the scattered intensity is reproduced by the RP theory at least qualitatively.

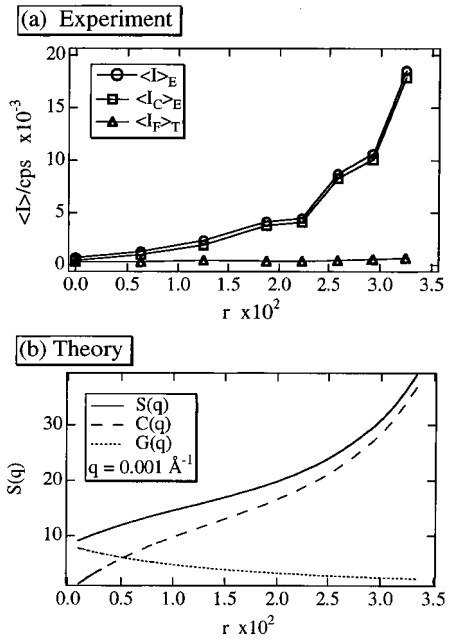

Figure 4. Cross-link density dependence of the scattered intensities, where r is the ratio of the concentrations of the cross-linker (BIS) to the monomer (NIPA), $r \equiv C_{BIS}/C_{NIPA}$. (a) Experimental results on $\langle I\rangle_E$, $\langle I_C\rangle_E$, and $\langle I_F\rangle_T$. (b) Calculated $S(q)$, $C(q)$, and $G(q)$ for gels with the parameter set of $f = f_0 = 0$, $\phi = \phi_0 = 0.078$, and $N = 1/r$.

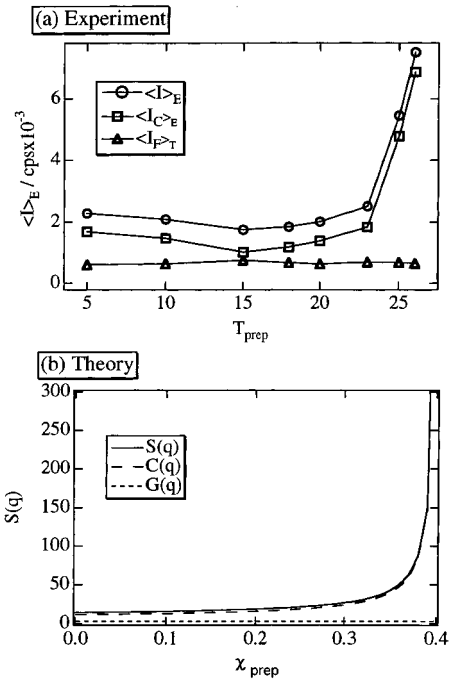

Figure 5. Preparation temperature, T_{prep}, dependence of (a) $\langle I\rangle_E$, $\langle I_C\rangle_E$, and $\langle I_F\rangle_T$ for NIPA homopolymer gels and (b) calculated χ_{prep} dependence of $S(q)$, $C(q)$, and $G(q)$ at $q = 0.001$ Å^{-1} with the parameter set of $f = f_0 = 0$, $\phi = \phi_0 = 0.078$, $N = 40$, and $\chi = 0.5$.

Figure 5a shows the preparation temperature, T_{prep}, dependence of $\langle I\rangle_E$, and $\langle I_C\rangle_E$, and $\langle I_F\rangle_T$ for NIPA homopolymer gels.[19] By increasing T_{prep}, both $\langle I\rangle_E$ and $\langle I_C\rangle_E$ increase, while $\langle I_F\rangle_T$ remains constant. The increase in $\langle I\rangle_E$ and $\langle I_C\rangle_E$ results from the fact that the system approaches its Θ temperature (~33 °C) and the contribution of the static inhomogeneities becomes dominant at preparation. On the other hand, the invariance of $\langle I_F\rangle_T$ with respect to T_{prep} is due to the fact

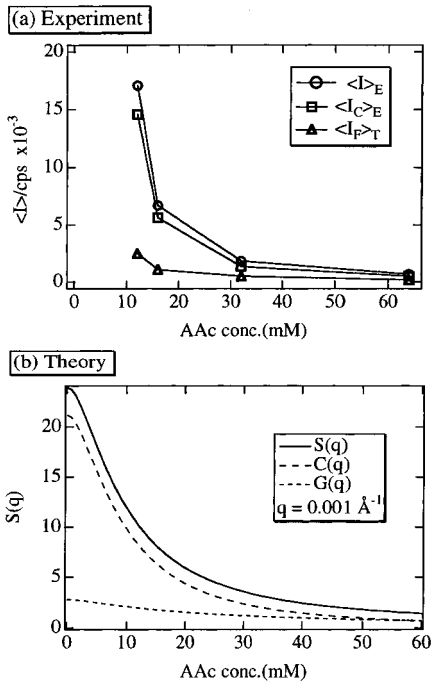

Figure 6. Degree of ionization, f, dependence of (a) $\langle I\rangle_E$, $\langle I_C\rangle_E$, and $\langle I_F\rangle_T$ for NIPA/AAc weakly charged gels prepared at 20 °C and observed at 20 °C and (b) calculated $S(q)$, $C(q)$, and $G(q)$ for gels with the parameter set of $N = 40$, $\chi = 0.5$, and $\phi = \phi_0 = 0.078$.

that this is one of the dynamic properties and is dependent not on T_{prep} but on the temperature at observation, T_{obs}. In Figure 5b, the χ_{prep} dependence of $S(q)$ was evaluated by using

$$w_0(q) = (1 - 2\chi_{prep} + \phi_0)\phi_0 N + \frac{\hat{l}_B f_0^{\,2}\phi_0 N^2}{Q^2(\phi_0/\phi)^{2/3} + \hat{l}_B f_0 \phi_0 N} \tag{19}$$

which is a modification of eq 10 for poor solvent systems. As shown in the figure, the behavior is again nicely reproduced by the theory at least qualitatively, while the variation of χ_{prep} is not correctly related to that of T_{prep}. The values employed for this simulation were $f = f_0 = 0$, $\phi = \phi_0 = 0.078$, $N = 40$, and $\chi = 0.5$.

Figure 6a shows the degree of ionization dependence of $\langle I\rangle_E$, $\langle I_C\rangle_E$, and $\langle I_F\rangle_T$ for NIPA/AAc weakly charged gels prepared at 20 °C and observed at 20 °C. With increasing f ($\equiv C_{AAc}/(C_{NIPA} + C_{AAc})$), both of the intensity components and the total intensity decrease, where C_{NIPA} and C_{AAc} are the NIPA and AAc monomer concentrations, respectively. These are accounted for by an increase in the osmotic pressure of the gel as a result of an increase of Donnan potential. Again, the f dependence is well recovered by the RP theory as shown in Figure 6b with the parameter set of $N = 40$, $\chi = 0.5$, and $\phi = \phi_0 = 0.078$. It should be pointed out here that the effect of charges is quite large to suppress scattering intensity. Particularly, the scattering due to the frozen inhomogeneities is significantly reduced by about 5 mol % of AAc to NIPA ($f \approx 0.05$). This finding is very important to design high transparent gels for application, such as contact lenses.

Figure 7a shows the variations of $\langle I\rangle_E$, $\langle I_C\rangle_E$, and $\langle I_F\rangle_T$ with T_{obs} in the poor solvent regime for NIPA/AAc (668 mM/32 mM) gel prepared at 20 °C. The χ ($\equiv\chi_{obs}$) values

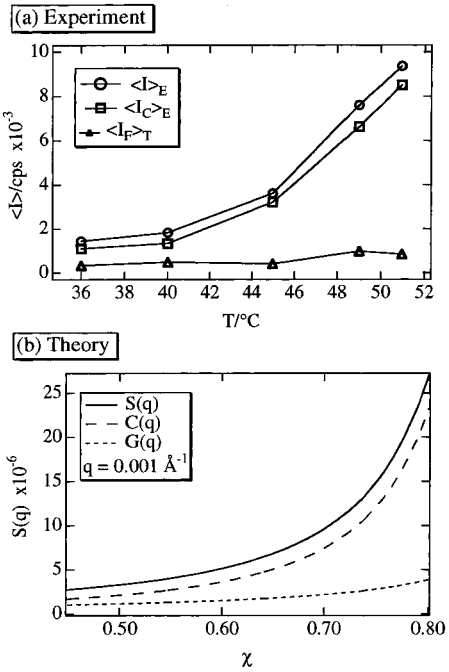

Figure 7. Observed temperature, T ($\equiv T_{obs}$), dependence of (a) $\langle I\rangle_E$, $\langle I_C\rangle_E$, and $\langle I_F\rangle_T$ of NIPA/AAc (668 mM/32 mM) gel prepared at 20 °C and (b) calculated $S(q)$, $C(q)$, and $G(q)$ for gels with the parameter set of $f = f_0 = 0.0457$, $\phi = \phi_0 = 0.078$, and $N = 40$.

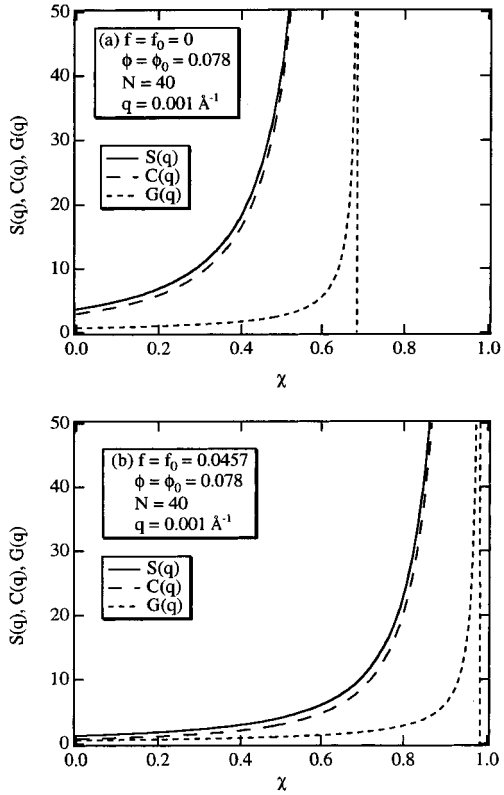

Figure 8. χ dependence of $S(q)$ (solid line), $C(q)$ (dashed lines), and $G(q)$ (dotted lines), near the critical χ ($\equiv\chi_c$), respectively, for (a) neutral gels ($f = 0$) and (b) weakly charged gels ($f = 0.0457$).

are chosen on the basis of the SANS curve fitting result (see Figure 2). Due to the increase of χ, both $\langle I\rangle_E$ and $\langle I_C\rangle_E$ increase considerably, which is in good accordance with the SANS result, i.e., the increase in $S(q)$ with T. This result of LS is again well reproduced by the theory as shown in Figure 7b. The preset parameters were $f = f_0 = 0.0457$, $\phi = \phi_0 = 0.078$, and $N = 40$. This result indicates that the estimated values of χ obtained by the SANS experiment seem to be relevant to account for the variation of the LS intensities with temperature for both dynamic and static aspects.

It is interesting to discuss the asymptotic behavior of the scattered intensities at higher temperatures. According to the previous LS study,[23] NIPA/AAc (668 mM/32 mM) has a spinodal temperature at 53.1 ± 0.5 °C, where the scattered intensity diverges. The theoretical prediction disclosed here indicates that this divergence is dominantly due to the divergence not of $\langle I_F\rangle_T$ (or $G(q)$) but of $\langle I_C\rangle_E$ (or $C(q)$). Note that the BE theory for polyelectrolyte solutions, where no static inhomogeneities are assumed, also predicts divergence of the structure factor by increasing χ. As a matter of fact, the presence of such divergence in the scattered intensity as well as the correlation length has been observed by SANS for neutral polymer solutions.[30] Figure 8 shows the comparison of the structure factors, $S(q)$, $C(q)$, and $G(q)$ for (a) neutral gels and (b) weakly charged gels. The employed parameters are shown in the Figures. All of $S(q)$, $C(q)$, and $G(q)$ diverge at $1 + w(q)g(q) = 0$. For simplicity, let us assume $q = 0$ and $\phi = \phi_0$ and calculate the critical χ ($\equiv\chi_c$) at which these correlators diverge, which is given by

$$\chi_c = \frac{1}{2}\left\{1 + \phi + \frac{1}{\phi}\left(\frac{1}{Ng(0)} + f\right)\right\} \approx \frac{1}{2}\left(1 + \phi + \frac{f}{\phi}\right) \quad (\text{for } N \gg 1) \quad (20)$$

In Figure 8a, χ_c is located at $\chi = 0.685$, which is somewhat larger than the calculated value of $\chi_c = 0.539$ for $\phi = \phi_0 = 0.078$. This disagreement is due to the employment of a finite N (=40) and q ($q = 0.001$ Å^{-1}) for the calculation. The important finding here is that $C(q)$ increases much faster than $G(q)$ with increasing χ although both diverge at χ_c. This is simply due to the presence of the squared term of in the denominator in $C(q)$, i.e., $\{1 + w(q)g(q)\}^2$, while $G(q)$ has $\{1 + w(q)g(q)\}$. This is why $C(q)$ and consequently $S(q)$ increase more dominantly with χ than $G(q)$. Therefore, the results shown in Figures 7 and 8 indicate that the static correlator is more sensitive to divergence than the dynamic correlator. This is also true for the case of weakly charged gels, where χ_c values shift toward a higher χ as predicted by eq 20.

All of these results clearly suggest that the scattered intensities can be decomposed to those ascribed to the static inhomogeneities and the dynamic fluctuations and those parameter dependencies are well predicted by the RP theory. As for the temperature dependence of the SANS scattered intensity functions for the weakly charged gels, $I(q)$'s are quantitatively reproduced by the RP theory, except for the gels having high concentrations. Though further investigations are necessary to understand the structure and dynamic properties of gels, the present study indicates that the RP theory well describes the characteristic feature of weakly charged gels.

As pointed out by Bastide and Leibler,[31] the contribution of the static inhomogeneities to the scattered intensity becomes dominant as the gel is deformed isotropically (e.g., swelling) or anisotropically (e.g., uniaxial deformation). Particularly, in the case of the latter, the problem is related to the so-called butterfly

pattern in the two-dimensional SANS intensity contour map. Though this problem has been solved by the experimental study by Rouf et al.[32] for noncharged polymer gels, that for weakly charged gels is quite interesting. Studies along this line were made by Skouri et al.[15] and Nisato et al.[17] mainly on the anisotropy in mechanical and osmotic properties. Recently we carried out a SANS study on weakly charged gels in deformed state and analyzed the two-dimensional scattering profiles with the RP theory, of which results have been reported elsewhere.[33]

Concluding Remarks

The experimental structure factors for temperature sensitive polymer gels obtained by SANS and DLS have been compared by the theoretical structure factors proposed by Rabin and Panyukov. By investigating the gel parameters, such as temperatures at preparation and at observation, T_{prep} and T_{obs}, cross-link density ($\sim 1/N$), and degree of ionization, f, the following facts were disclosed:

(1) The observed static structure factor, $I(q)$, by SANS was quantitatively fitted with the Rabin−Panyukov theory for randomly cross-linked weakly charged gels. The estimated values of χ by the curve fitting varied reasonably with temperature and polymer volume fraction as long as the fitting was satisfactory. This accordance between the experimental observation and the theoretical prediction on the static structure factor indicates that the origin of the scattering peak appearing at elevated temperatures (>43 °C) is mainly due to the static inhomogeneities.

(2) The experimental results of the parameter dependence obtained by DLS elucidate the relationship between the gel parameters, such as T_{prep}, T_{obs}, N, and f, and the structure factors, the static inhomogeneities $\langle I_C \rangle_E$, and the dynamic fluctuations $\langle I_F \rangle_T$ are satisfactorily predicted with the RP theory as the variations of the static $C(q)$ and dynamic $G(q)$ correlators, respectively. It is now clear that the static inhomogeneities are inherent in the concentration fluctuations in gels and play a major role in the scattering behavior both in the SANS (on the order of a few hundred angstroms) and LS (on the order of a few micrometers) regimes. This is due to the topological restriction of the polymer chain concentration fluctuations by cross-linking.

(3) An introduction of charges to polymer networks effectively reduces the concentration fluctuations. In particular, the static inhomogeneities are remarkably suppressed by charges, which is in accordance with the report by Mossaid et al.[16] This effect is also well predicted by the theory.

(4) The static inhomogeneities, i.e., $\langle I_C \rangle_E$ (or $C(q)$), are more sensitive to divergence in $I(q)$ (or $S(q)$) than the dynamic fluctuations, $\langle I_F \rangle_T$.

Acknowledgment. This work is partially supported by the Ministry of Education, Science, Sports, and Culture, Japan (Grant-in-Aid, No. 09450362).

References and Notes

(1) Plestil, J.; Ostanevich, Y. M.; Borbely, S.; Stejskal, J.; Iravsky, M. *Polym. Bull.* **1987**, *17*, 465.
(2) Schosseler, F.; Ilmann, F.; Candau, S. J. *J. Phys. II, Fr.* **1991**, *1*, 1197.
(3) Shibayama, M.; Tanaka, T.; Han, C. C. *J. Chem. Phys.* **1992**, *97*, 6842.
(4) Borue, V.; Erukhimovich, I. *Macromolecules* **1988**, *21*, 3240.
(5) Moussaid, A.; Schosseler, F.; Munch, J. P.; Candau, S. J. *J. Phys. II, Fr.* **1993**, *3*, 573.
(6) Panyukov, S.; Rabin, Y. *Phys. Rep.* **1996**, *269*, 1.
(7) Panyukov, S.; Rabin, Y. *Macromolecules* **1996**, *29*, 7960.
(8) Rabin, Y.; Panyukov, S. *Macromolecules* **1997**, *30*, 301.
(9) Candau, S. J.; Toung, C. Y.; Tanaka, T.; Lemarechal, P.; Bastide, J. *J. Chem. Phys.* **1979**, *70*, 4694.
(10) Mallam, S.; Hecht, A. M.; Geissler, E. *J. Chem. Phys.* **1989**, *91*, 6447.
(11) Mallam, S.; Horkay, F.; Hecht, A. M.; Geissler, E. *Macromolecules* **1989**, *22*, 3356.
(12) Pusey, P. N.; van Megen, W. *Physica A* **1989**, *157*, 705.
(13) Joosten, J. G. H.; McCarthy, J. L.; Pusey, P. N. *Macromolecules* **1991**, *24*, 6690.
(14) Xue, J. Z.; Pine, D. J.; Milner, S. T.; Wu, X. L.; Chaikin, P. M. *Phys. Rev. A* **1991**, *46*, 6550.
(15) Skouri, R.; Muhch, J. P.; Schosseler, F.; Candau, S. J. *Europhys. Lett.* **1993**, *23*, 635.
(16) Moussaid, A.; Candau, S. J.; Joosten, J. G. H. *Macromolecules* **1994**, *27*, 2102.
(17) Nisato, G.; Skouri, R.; Schosseler, F.; Munch, J.-P.; Candau, S. J. *Faraday Discuss.* **1995**, *101*, 133.
(18) Shibayama, M.; Norisuye, T.; Nomura, S. *Macromolecules* **1996**, *29*, 8746.
(19) Shibayama, M.; Takata, T.; Norisuye, T. *Physica A*, in press.
(20) Shibayama, M. *Macromol. Chem. Phys.*, in press.
(21) Higgins, J. S.; Benoit, H. C. *Polymers and Neutron Scattering*; Clarendon Press: Oxford, England, 1994.
(22) Tanaka, T.; Hocker, L. O.; Benedek, G. B. *J. Chem. Phys.* **1973**, *59*, 5151.
(23) Shibayama, M.; Fujikawa, Y.; Nomura, S. *Macromolecules* **1996**, *29*, 6535.
(24) Kubota, K.; Fujishige, S.; Ando, I. *Polym. J.* **1990**, *22*, 15.
(25) Ikkai, F.; Shibayama, M. *Phys. Rev. E* **1997**, *56*, R51.
(26) Shibayama, M.; Ikkai, F.; Shiwa, Y.; Rabin, Y. *J. Chem. Phys.* **1997**, *107*, 5227.
(27) Ikkai, F.; Shibayama, M.; Nomura, S.; Han, C. C. *Macromolecules*, submitted.
(28) Shibayama, M.; Tanaka, T. *J. Chem. Phys.* **1995**, *102*, 9392.
(29) Shibayama, M.; Ikkai, F.; Inamoto, S.; Nomura, S.; Han, C. C. *J. Chem. Phys.* **1996**, *105*, 4358.
(30) Shibayama, M.; Tanaka, T.; Han, C. C. *J. Chem. Phys.* **1992**, *97*, 6829.
(31) Bastide, J.; Leibler, L. *Macromolecules* **1988**, *21*, 2647.
(32) Rouf, C.; Bastide, J.; Pujol, J. M.; Schosseler, F.; Munch, J. P. *Phys. Rev. Lett.* **1994**, *73*, 830.
(33) Shibayama, M.; Kawakubo, K.; Ikkai, F. *Macromolecules*, submitted.

MA971641Q